Spectrochimica Acta Part A: Molecular and Biomolecular Spectroscopy 290 (2023) 122259

Contents lists available at ScienceDirect

Spectrochimica Acta Part A: Molecular and Biomolecular Spectroscopy

journal homepage: www.journals.elsevier.com/spectrochimica-acta-part-a-molecular-and-biomolecular-spectroscopy

Monitoring glucose levels in urine using FTIR spectroscopy combined with univariate and multivariate statistical methods

Douglas Carvalho Caixeta [a,1], Cassio Lima [b,c,1], Yun Xu [c], Marco Guevara-Vega [a], Foued Salmen Espindola [d], Royston Goodacre [c], Denise Maria Zezell [b], Robinson Sabino-Silva [a,*]

[a] Innovation Center in Salivary Diagnostics and Nanobiotechnology, Department of Physiology, Institute of Biomedical Sciences, Federal University of Uberlandia, Uberlandia, Brazil
[b] Center for Lasers and Applications, Nuclear and Energy Research Institute, IPEN-CNEN/SP, São Paulo, Brazil
[c] Centre for Metabolomics Research, Department of Biochemistry and Systems Biology, Institute of Systems, Molecular and Integrative Biology, University of Liverpool, United Kingdom
[d] Institute of Biotechnology, Federal University of Uberlandia, Uberlandia, Brazil

HIGHLIGHTS

- Urinary spectral of FTIR with univariate and multivariate statistical can use for diabetes surveillance.
- Spectral of urine analysis exhibited consistent changes related to urea, creatinine, and glucose.
- The 100 % accuracy of glucose (1074 cm^{-1}) and strong correlation with glycosuria can discriminate the urine of diabetics.
- MCR-ALS analysis suggested that glucose prediction could be helpful in the screening and monitoring of diabetes.

GRAPHICAL ABSTRACT

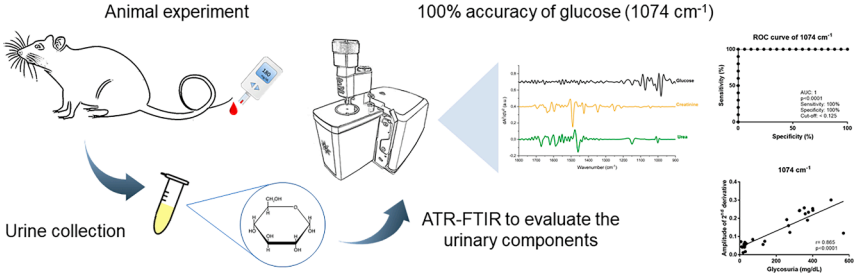

ARTICLE INFO

Keywords:
Diabetes
ATR-FTIR
Urinary biomarkers
Chemometrics analysis

ABSTRACT

The development of novel platforms for non-invasive continuous glucose monitoring applied in the screening and monitoring of diabetes is crucial to improve diabetes surveillance systems. Attenuated total reflection-Fourier transform infrared (ATR-FTIR) spectroscopy of urine can be an alternative as a sustainable, label-free, fast, non-invasive, and highly sensitive analysis to detect changes in urine promoted by diabetes and insulin treatment. In this study, we used ATR-FTIR to evaluate the urinary components of non-diabetic (ND), diabetic (D), and diabetic insulin-treated (D + I) rats. As expected, insulin treatment was capable to revert changes in glycemia, 24-h urine collection volume, urine creatinine, urea, and glucose excretion promoted by diabetes. Several differences in the urine spectra of ND, D, and D + I were observed, with urea, creatinine, and glucose analytes being related to these changes. Principal components analysis (PCA) scores plots allowed for the discrimination of ND and D + I from D with an accuracy of ~ 99 %. The PCA loadings associated with PC1 confirmed the

* Corresponding author at: Federal University of Uberlandia (UFU), Institute of Biomedical Sciences (ICBIM), ARFIS, Av. Pará, 1720, Campus Umuruama, CEP 38400-902, Uberlandia, MG, Brazil.
E-mail addresses: caixetadoug@gmail.com (D.C. Caixeta), Cassio.Lima@liverpool.ac.uk (C. Lima), Yun.Xu@liverpool.ac.uk (Y. Xu), marco.guevara.vega@gmail.com (M. Guevara-Vega), foued@ufu.br (F.S. Espindola), roy.goodacre@liverpool.ac.uk (R. Goodacre), zezell@gmail.com (D.M. Zezell), robinsonsabino@ufu.br (R. Sabino-Silva).
[1] Both authors contributed equally to this work.

https://doi.org/10.1016/j.saa.2022.122259
Received 29 July 2022; Received in revised form 12 December 2022; Accepted 16 December 2022
Available online 17 December 2022
1386-1425/© 2022 Published by Elsevier B.V.

importance of urea and glucose vibrational modes for this discrimination. Univariate analysis of second derivative spectra showed a high correlation (r: 0.865, $p < 0.0001$) between the height of 1074 cm-1 vibrational mode with urinary glucose concentration. In order to estimate the amount of glucose present in the infrared spectra from urine, multivariate curve resolution-alternating least square (MCR-ALS) was applied and a higher predicted concentration of glucose in the urine was observed with a correlation of 78.9 % compared to urinary glucose concentration assessed using enzyme assays. In summary, ATR-FTIR combined with univariate and multivariate chemometric analyses provides an innovative, non-invasive, and sustainable approach to diabetes surveillance.

1. Introduction

Diabetes mellitus (DM) is a chronic metabolic disorder characterized by hyperglycemia related to damage in insulin secretion by pancreatic β-cells and/or reduced insulin action on target tissues [1]. It is estimated that around 537 million people worldwide live with DM [2]. Approximately 90 % are affected by type 2 diabetes and 10 % by type 1 diabetes [2]. This endocrine disorder is a global health issue and presents higher health costs for surveillance and treatment. Tight control of glycemic levels is critical to reduce morbidity and mortality in diabetic patients. In this context, alternative methods to assess metabolic control are critical to prevent long-term complications and to improve the quality of life in individuals with diabetes [3,4].

Diabetes affects multiple organs, and it is the leading cause of kidney dysfunctions 6. Polyuria and changes in urinary composition including glucose, creatinine, and urea are present in people with diabetes. Diabetes treatment with optimal glycemic control is capable to suppress these diabetic urinary parameters [5,6]. Urine is an attractive non-invasive fluid that has been frequently used to support clinical decisions for diabetic patients based on monitoring of renal function [5].

Attenuated total reflection-Fourier transform infrared (ATR-FTIR) spectroscopy is a powerful bioanalytical tool suitable to provide a sustainable, label-free, rapid, non-destructive, and relatively low-cost molecular component analysis in biofluids [7–9]. Over the past decades, research has been conducted in search of novel techniques that can monitor glucose levels in diabetic patients in a rapid, cost-effective, and non-invasive manner. Furthermore, FTIR technology is also available as portable devices, which is ideal for point-of-care medicine. ATR-FTIR is capable of measuring the specific vibrational modes resulting from carbohydrates, proteins, lipids, electrolytes, DNA, and RNA simultaneously and without extensive sample preparation [7,9]. The discrimination of healthy and pathological conditions, as well as the efficacy of treatments, has been widely performed by ATR-FTIR [10]. Urine-based spectroscopy infrared (IR) bands have already been applied successfully in several studies, for microproteinuria [11], bacteria causing urinary tract infections [12], endometrial and ovarian cancers [13,14], prostate and urogenital cancer [15,16], drug-induced crystalluria [17], primary hyperoxaluria [18], and many other diseases [19].

In order to open new avenues for the use of infrared spectroscopy on urine as a novel approach for personalized medicine, we hypothesized that ATR-FTIR is capable of identifying changes in urinary molecules altered by diabetes and thus reverted by appropriate insulin treatment. Therefore, the present study aims to demonstrate the ability of ATR-FTIR spectroscopy combined with univariate and multivariate curve resolution-alternating least square (MCR-ALS) analysis to monitor urinary parameters of non-diabetic and diabetic rats, as well as insulin-treated diabetic animals.

2. Material and methods

2.1. Animal experiment

All experiments were conducted following recommendations of the Brazilian Society of Laboratory Animals Science (SBCAL) in the guide for the care and use of laboratory animals. Experimental procedures for the handling, use, and euthanasia were approved by the Ethics Committee for Animal Research of the Federal University of Uberlandia (UFU) (License #CEUA-UFU No. 013/2016) according to Ethical Principles adopted by the Brazilian College of Animal Experimentation (COBEA) and conformed to ARRIVE guidelines.

Male Wistar rats (~260 g) were provided from the Center for Bioterism and Experimentation (REBIR) at the Federal University of Uberlandia. The animals were maintained under standard conditions (12-hour light/dark cycles, light on at 7 a.m.; 22 ± 2 °C; humidity ~ 60 %) and were allowed free access to water and a standard diet within this rodent facility.

Overnight-fasted animals received a single intraperitoneal injection (60 mg/kg) of streptozotocin (STZ) (Sigma-Aldrich, St. Louis, MO. USA) dissolved in 0.1 M citrate buffer (pH 4.5) to induce diabetes. Animals with hyperglycemia (>250 mg/dL) 48 h later were considered diabetics (D). Non-diabetic (ND) animals received injection of 0.9 % NaCl (physiological saline) in similar volumes (n = 8). Thus, diabetic animals were divided in placebo-treated Diabetic (D, n = 10) and Diabetic treated with 6 U Insulin (D + I, n = 10). Subsequently, 21 days after diabetes induction, diabetic rats received treatment with vehicle (NaCl 0.9 % in D rats) or with 6 U of insulin [NPH insulin, Biobrás, MG, Brazil] (D + I) per day (2 U at 8:30 a.m. and 4U at 5:30p.m.) subcutaneously in D + I rats. ND animals also received vehicle (0.9 % NaCl) [20–22].

2.2. Urine sample collection and preparation

On day 6 of treatment, the rats were maintained for 24-hours in metabolic cages to allow for 24 h-urine collection from each animal separately. The samples were collected, measured, processed, and stored at −80 °C until further analysis. Creatinine, urea, and glucose concentration in the urine were measured using enzymatic assays following the manufacturer's instructions (Labtest Diagnostica SA, Brazil). Blood glucose levels obtained from the tail vein were measured in overnight-fasted animals using reactive strips for glucometer (Accu-Chek Performa, Roche Diagnostic Systems, Basel, Switzerland). Besides that, the variation of gain/loss body weight (Δ body weight) after STZ or placebo administration was analysed. Animals were euthanized with an excessive anesthetic dose immediately after sample collections.

After that, urine samples were lyophilized (L101, Liotop®) and the samples were analysed after drying.

2.3. FTIR spectroscopy and data analysis

Infrared spectra were acquired using an FTIR system (Nicolet 6700, Thermo Scientific, Waltham, MA, USA) in Attenuated Total Reflectance (ATR) mode over the range 4000–400 cm^{-1}. Spectra were recorded with a spectral resolution of 4 cm^{-1} and 100 scans (co-adds) per spectrum. FTIR spectra were smoothed via Savitzky-Golay filter (polynomial of second order in an eleven-point window), followed by rubberband baseline correction, and vector normalized prior to spectra data analysis. The fingerprint region (1800–900 cm^{-1}) was used as the input to PCA and MCR-ALS techniques [23]. All pre-processing steps and spectral analyses were performed using Matlab® R2019b (MathWorks, Natick, MA, USA) and all computational algorithms are available in Github (https://github.com/Biospec/). In addition, second derivative spectra were obtained by applying Savitzky-Golay algorithm with polynomial order 5 and 20 points of the window.

2.4. Glucose, creatinine, and urea and sample preparation

Glucose, creatinine and urea (>99.0 %) were purchased from Sigma-Aldrich (Sigma-Aldrich Dorset, UK). The experiments to analyze the infrared spectra of these molecules, were conducted in a similar protocol as described to urine. Aqueous solutions of glucose (800 mM), creatinine (500 mM), and urea (850 mM) were transferred onto ATR crystal and left to dry at room temperature before data collection.

2.5. Statistical analysis

The normality of data distribution was analyzed using the Kolmogorov-Smirnov test. The amplitude of second derivatives were analyzed using one-way analysis of variance (ANOVA), followed by Tukey Multiple Comparison as a post-hoc test. Receiver Operating Characteristic (ROC) curve and Pearson correlation test were applied for all second derivative peaks intensity. All these analyses were performed using the software GraphPad Prism (GraphPad Prism version 7.00 for Windows, GraphPad Software, San Diego, CA, USA). Only values of $p < 0.05$ were considered significant and the results were expressed as mean ± S.D.

3. Results and discussion

The DM and insulin treatment effects on animals were characterized by several parameters, which are shown in Table 1. As expected, a reduction in weight gain ($p < 0.05$), an increase in plasmatic glycemic levels ($p < 0.05$) and higher 24 h-urinary volume ($p < 0.05$) were observed in D compared with ND rats. By contrast, no change in the concentration of urinary creatinine was observed; however, 24 h urinary creatinine excretion was increased ($p < 0.05$) in D compared to ND. In addition, the urinary urea concentration decreased ($p < 0.05$) in D compared to ND, and its level in 24 h urinary urea excretion increased ($p < 0.05$) in D compared to ND rats. Both glucose concentration in urine and 24 h urinary glucose excretion were also higher ($p < 0.05$) in D compared to ND.

Insulin treatment resulted in weight gain ($p < 0.05$) with concomitant reduction in plasma glucose levels ($p < 0.05$) and urinary volume ($p < 0.05$) compared to D rats. Creatinine levels in urine did not change during insulin treatment; however, 24 h urinary creatinine excretion decreased ($p < 0.05$) in D + I compared to D rats. Regarding urea concentration in urine, insulin treatment was not efficient to restore ($p > 0.05$) this parameter. On the other hand, insulin treatment reduced ($p < 0.05$) 24 h urinary urea excretion compared to D rats. As expected, the urinary glucose concentration and 24 h urinary glucose excretion were lower ($p < 0.05$) in D + I compared to D rats (Table 1). Bearing in mind the classical effects of insulin treatment on urinary parameters, diabetic animals treated with insulin or placebo showed similar metabolic profiles as described in previous studies, in which urinary parameters were changed by diabetes induction, and those parameters were restored to normoglycemic profile with insulin treatment [20,24–26].

Table 1
Effect of diabetes and insulin on body weight, glycemia, 24 h urinary volume, urinary creatinine concentration, 24 h urinary creatinine excretion, urinary urea concentration, 24 h urinary urea excretion, glycosuria and 24 h urinary glucose excretion.

Parameters	ND	D	D + I
Δ Body weight (g)	51.6 ± 24.9	−20.1 ± 37.4*	23.2 ± 31.5#
Glycemia (mg/dL)	83.7 ± 13.4	483.8 ± 59.9*	102.4 ± 100.8#
24 h urinary volume (mL)	23.2 ± 10.4	124.2 ± 31.0*	35.1 ± 12.7#
Urinary creatinine concentration (md/dL)	0.52 ± 0.15	0.62 ± 0.28	0.65 ± 0.33
24 h urinary creatinine excretion (mg/24 h)	12.6 ± 8.2	76.7 ± 40.0 *	20.7 ± 8.1#
Urinary urea concentration (md/dL)	94.6 ± 56.0	35.1 ± 9.0*	38.4 ± 15.5*
24 h urinary urea excretion (mg/24 h)	20.9 ± 14.9	44.0 ± 16.6 *	12.5 ± 5.4#
Glycosuria (mg/dL)	24.7 ± 20.3	367.8 ± 62.8*	165.5 ± 181.3*#
24 h urinary glucose excretion (mg/24 h)	4.6 ± 2.6	461.3 ± 173.4*	51.9 ± 58.3#

Values are expressed as mean ± S.D.
* $p < 0.05$ vs ND rats;
# $p < 0.05$ vs D rats. Non-diabetic rats (ND), Diabetic rats (D) and Diabetic rats with insulin treatment (D + I).

Infrared spectra from urine collected using ATR-FTIR are complex signatures and these biochemical fingerprints are related to the many infrared-active molecules within this complex biological mixture. Water is the main component of urine (over 95 %) and due to its strong absorption bands in the mid-infrared region, the samples must be dry before ATR-FTIR analysis to generate signals from the signatures of molecules in lower concentrations [9]. Fig. 1 shows the fingerprint region (1800–900 cm^{-1}) of spectra acquired from lyophilized urine of non-diabetic and diabetic rats, as well as, the spectra of pure glucose, creatinine, and urea.

The spectral signatures observed in both urinary spectra in non-diabetic and diabetic conditions are linear combinations of the individual spectra from the individual urinary constituents. Urea is an important component in urine (Table 1) and other constituents include creatinine, uric acid, organic and inorganic salts, proteins, hormones, and other metabolites. Spectra of urea and creatinine are also shown in Fig. 1 due to their abundance in urine as well as their clinical relevance. Urea is a relatively small molecule with the molecular formula of NH_2CONH_2, it is therefore not surprising that the IR spectrum of urea is relatively simple and has distinct bands at 1149 cm^{-1} (NH rocking vibrations), 1459 cm^{-1} (antisymmetric CN stretch), 1587 cm^{-1} (CO stretch), 1620 cm^{-1} (antisymmetric NH bend), and 1671 cm^{-1} (symmetric NH bend) [27]. The IR spectrum of creatinine ($C_4H_7N_3O$) depicts bands peaking at 1490 cm^{-1} (C═N stretch, CN stretch, NCH bend) and three bands between 1500 and 1700 cm^{-1} [28]. It is important to notice that urea and creatinine molecules strongly interact with water due to hydrogen bonding with N—H, therefore the IR spectra of both compounds are different in aqueous solution compared to fully dried states. Oliver, Maréchal and Rich [29] demonstrated that the antisymmetric C—N stretch (ν_{as}(CN)) vibration from urea, which is found at 1468 cm^{-1} in aqueous solution, shifts to 1464 cm^{-1} when urea is completely dry. However, two additional states of urea with ν_{as}(CN) peaks at 1454 cm^{-1} or 1443 cm^{-1} were also observed in partially hydrated samples [29]. Thus, IR spectra interpretation of such molecules must be performed with caution since the intermediate forms due to different degrees of hydration may be present when whole urine is dried. According to Fig. 1, bands from 1700 cm^{-1} to 1400 cm^{-1} in spectra collected from urine of both healthy and diabetic rats are mainly due to urea and creatinine.

The exact constitution of urine changes with lifestyle and health status for each individual. Hence, some diseases can result in elevated levels of certain urine components. It is well known that diabetic patients present elevated glucose levels in urine (glycosuria). IR signatures of glucose are also shown in Fig. 1 and these vibrations spectral features are mainly dominated by C—O and C—O—C stretching resulting in peaks in the low wavenumber region (900–1200 cm^{-1}) [30,31]. The low wavenumber region of spectra from diabetic rats is dominated by vibrations related to glucose, which indicates elevated glycosuria. These features are very small in infrared spectra collected from healthy non-diabetic rats (Fig. 1).

Spectra from healthy and non-diabetic animals were subjected to PCA in order to evaluate any specific separation related to the development of diabetes. The resultant PCA scores plot (Fig. 2A) displayed a clear separation between spectral data acquired from healthy and diabetic animals. Scores related to healthy rats were grouped on the

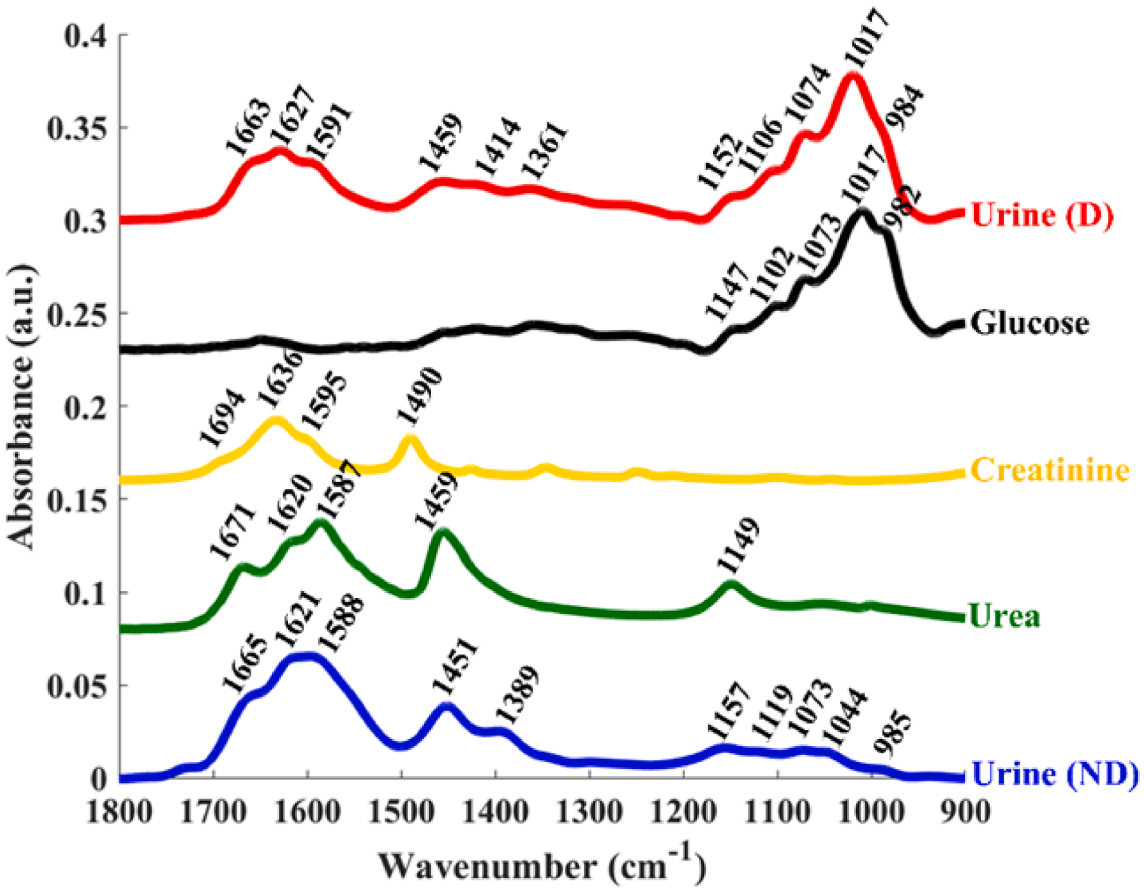

Fig. 1. Fingerprint region (1800–900 cm^{-1}) of typical infrared spectra of urine collected from healthy (ND, blue), diabetic (D, red), along with the spectra from pure urea (green), creatinine (yellow), and glucose (black). Peaks are highlighted which are discussed in the text.

negative side of the first principal component (PC-1) axis, while diabetic animals were clustered on the positive side. PC-1 which accounts for 98 % of the total explained variance (TEV), retains information responsible for the clustering pattern obtained in the scores plot. The corresponding PC-1 loadings are illustrated in Fig. 2B. Positive loadings on bands peaking at the low wavenumber region indicate the high glucose levels in urine of diabetic rats. On the other hand, negative loadings were observed for bands associated with other urinary constituents, indicating higher urea and creatinine content in urine of non-diabetic animals.

Fig. 3 illustrates spectra depicted for each D + I animal (n = 10), as well as averaged spectra of signatures acquired from all D and ND rats. Most spectra from insulin-treated diabetic animals (90 %) presented glucose bands at levels comparable to healthy animals, indicating a positive response to the treatment (D + I in green color). However, the spectrum from one D + I animal with reduced response to insulin treatment presented bands indicating high glucose content (D + I in orange color), indicating a profile similar to urine from non-treated diabetic animals. Similar findings were evidenced by PCA applied to all datasets in ND, D, and D + I rats. PCA scores related to D + I animals were grouped on the same cluster of ND animals, indicating a positive response to insulin (Fig. 2C). On the other hand, PCA scores associated with the animal with high urinary glucose content were grouped within the cluster containing scores from untreated diabetic animals. PC-1 loadings are shown in Fig. 2D and illustrate similar findings to PC-1 loadings depicted in Fig. 2C. These findings indicate the ability of urinary ATR-FTIR spectroscopy as a rapid screening platform for diabetes as well as a tool to evaluate the metabolic response of diabetic patients to insulin treatment.

We also calculated the second derivative of ATR-FTIR spectrum to amplify the spectral variations of the urinary components glucose, creatinine, and urea (Fig. 4A) and compared these with ND, D, and D + I rats (Fig. 4B).

The second derivative analysis is capable to enhance the separation of overlapping vibrational modes. Relative changes in the amplitude of second derivative are related to the presence of each component. In Fig. 4.A the amplitude of second derivatives for urea band peaking at 1452 cm^{-1} were reduced ($p < 0.05$) in the urine of D compared to ND rats, and the treatment with insulin was effective and caused increase ($p < 0.05$) in this amplitude compared to D rats. Considering that sensitivity and specificity are basic characteristics to determine the accuracy of diagnostic, triage, and monitoring tests [32–34], receiver operating characteristic (ROC) curve analyses were used to evaluate the potential of these spectral vibrational modes. In this context, we compared hyperglycemic (D) rats to normoglycemic ND and D + I, thus removing the sample of D + I due to the glycemia of 439 mg/dL representing a diabetic metabolic profile. The area under the curve (AUC) of ROC analysis based on amplitude of second derivative of the band peaking at 1452 cm-1 was 0.905 ($p < 0.0005$), and the best discrimination threshold value was 0.05282 with a sensitivity of 100 % and specificity of 88.2 %. However, no correlation was observed between these amplitude values and urinary urea concentrations ($r = -0.051$, $p = 0.798$) (Fig. 5A). In Fig. 5B the second derivative amplitudes of creatinine at 1490 cm-1 were reduced ($p < 0.05$) in the urine of D compared to ND rats, and the treatment with insulin increased ($p < 0.05$) this amplitude compared to D rats. The AUC of ROC analysis based on amplitude at 1490 cm-1 in the second derivative was 0.958 ($p < 0.0001$), and the cut-off value was 0.01105 with a sensitivity of 100 % and specificity of 88.2 %. Again, no correlation was observed between the amplitudes at 1490 cm^{-1} in second derivative with urinary creatinine ($r = -0.167$, $p = 0.405$) (Fig. 5B).

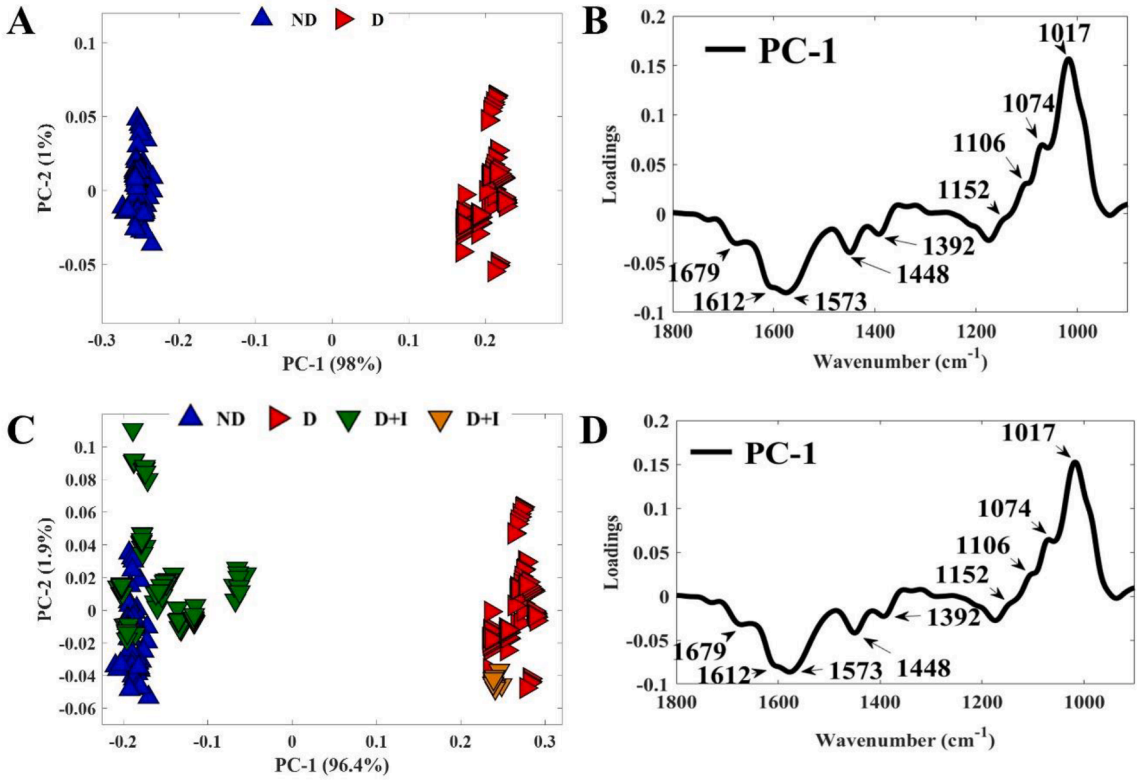

Fig. 2. PCA scores plots (A) and PC-1 loadings plots (C) obtained by applying PCA to FTIR spectra of urine acquired from healthy (ND) and diabetic (D) animals. PCA scores (C) and loadings (D) results obtained for FTIR spectra of urine acquired from healthy (ND), diabetic (D), and insulin-treated diabetic (D + I) rats. One D + I animal with glycemia of 439 mg/dL is highlighted in orange due to reduced effectiveness of insulin treatment on the diabetic metabolic profile.

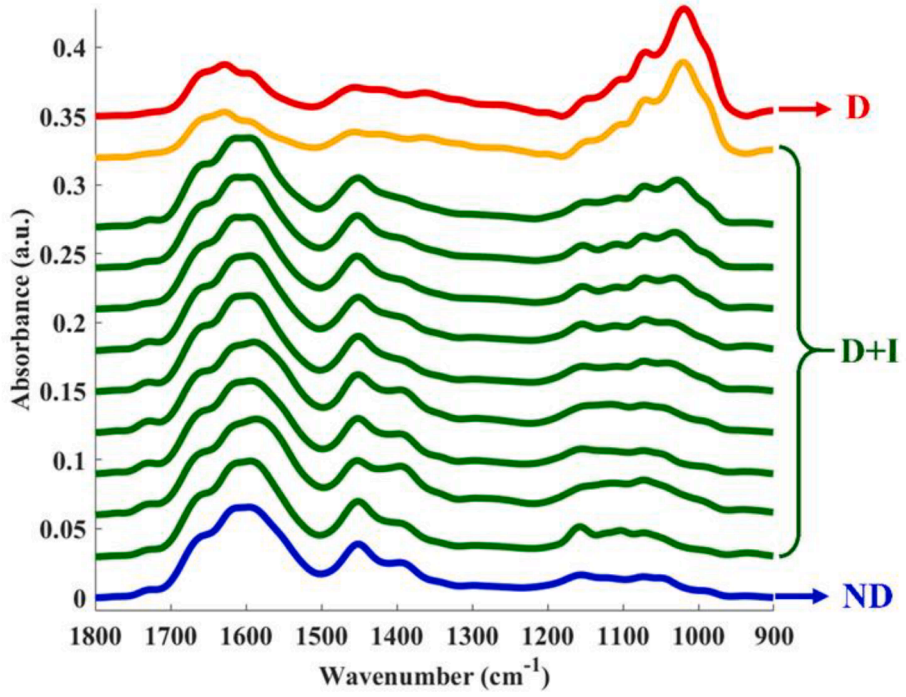

Fig. 3. Averaged FTIR spectra collected from the urine of each insulin-treated diabetic animal, as well as averaged spectra of signatures acquired from all diabetic (red) and non-diabetic rats (blue). Green lines relate to animals with positive response to insulin-treatment, while the orange line represents the animal that displayed no response to insulin treatment.

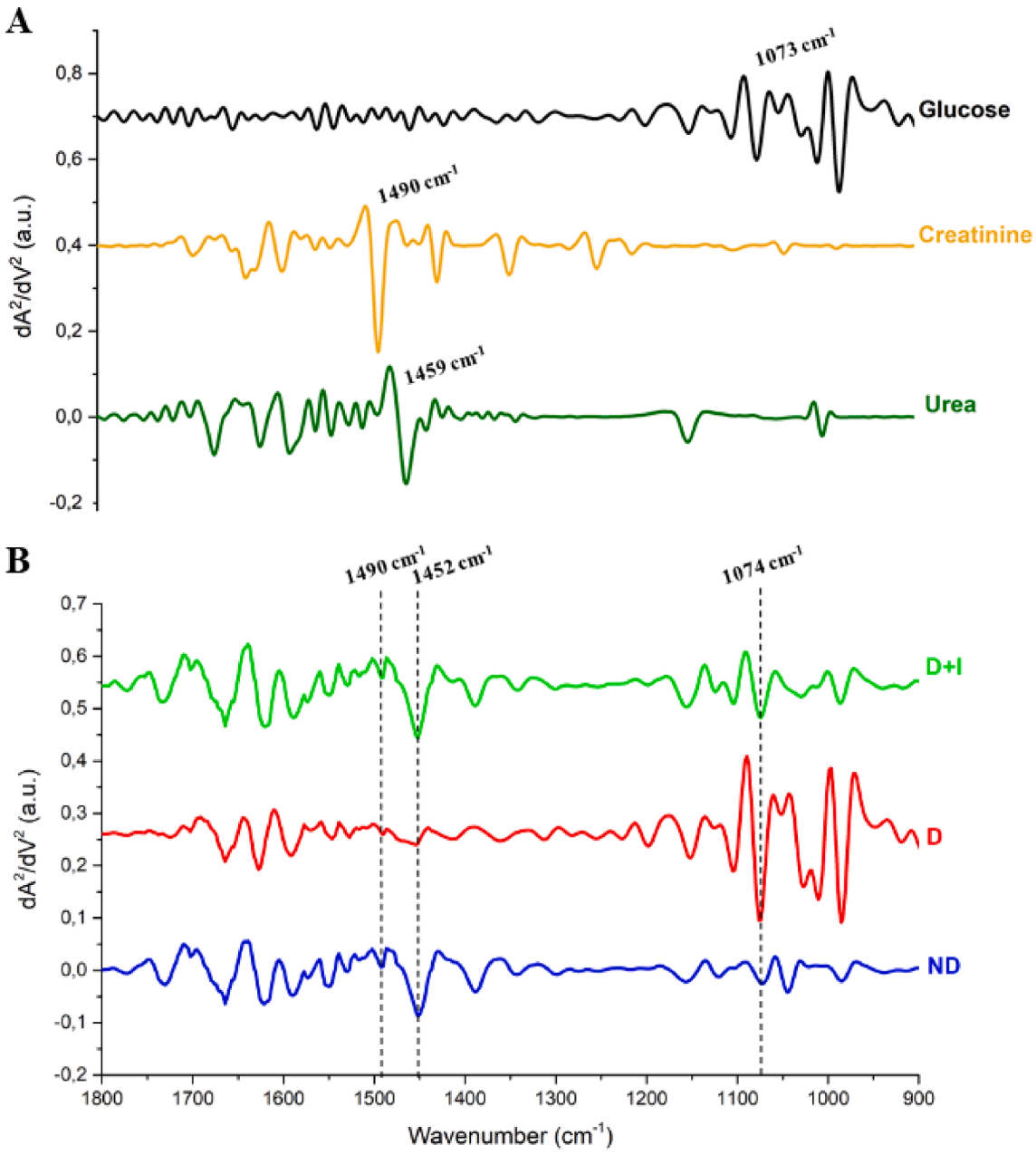

Fig. 4. Fingerprint region (1800–900 cm^{-1}) of urinary spectra from glucose (black), creatinine (yellow) and urea (green) (A) and non-diabetic (ND, blue), diabetic (D, red) and insulin-treated diabetic (D + I) rats (B).

Finally, in Fig. 5C the urinary amplitude of glucose at 1074 cm^{-1} was increased ($p < 0.05$) in D compared to ND rats, and the treatment with insulin effectively reduced ($p < 0.05$) this amplitude compared to D rats. The area under the curve (AUC) of ROC analysis based on amplitudes at 1490 cm^{-1} in the second derivative was 1.0 ($p < 0.0001$), and the selected discrimination threshold value was 0.125 with both sensitivity and specificity of 100 %. In this instance, the analysis of 1490 cm^{-1} amplitudes with glycosuria showed a strong and positive correlation ($r = 0.865$; $p < 0.0001$) (Fig. 5.C) indicating that the main change in the urine between ND and R rats was the level of glucose, which could be recovered in D + I when the rats were treated with insulin.

MCR-ALS is a popular modelling method used to deconvolve spectra from mixtures into their individual components. Thus, MCR-ALS was applied to infrared urinary spectra of ND, D, and D + I animals in order to estimate the relative concentrations of creatinine, urea, and glucose from the whole urine spectrum. MCR-ALS assumes that the recorded spectra are the weighted sum of pure spectra of the components present in the investigated mixture and returns the resolved spectrum of each compound as well as its concentration in the mixture spectrum. Fig. 6A shows a good correlation of FTIR spectrum of laboratory-grade commercial glucose (blue line) to the resolved (pure) spectrum obtained through MCR-ALS. Thus, this approach can be applied to estimate the relative concentration of glucose in urine spectra. Fig. 6B shows a scatter plot of glucose concentration estimated by MCR-ALS plotted against glucose levels in urine obtained via enzymatic kits. Linear regression showed a positive correlation between glucose levels obtained through MCR-ALS and enzymatic kits ($R2 = 0.7893$). By contrast, MCR-ALS was not able to reproduce the signatures of urea and creatinine (data not shown), which may have occurred due to the different hydration degree of spectral signatures obtained from pure compounds compared to signatures of both molecules in urine.

Glucose and other monosaccharides absorb are detected at

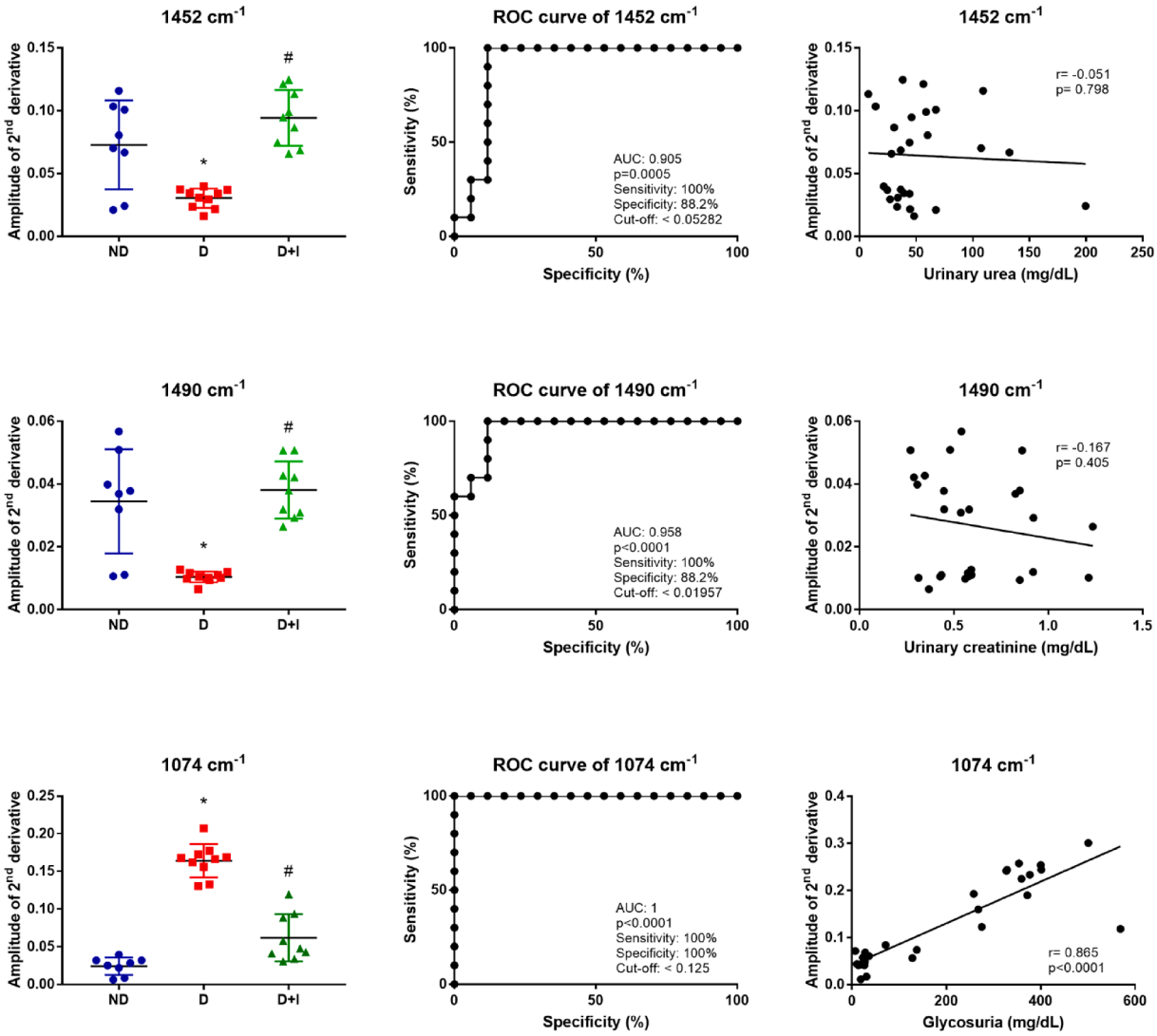

Fig. 5. Analyses of three key peaks seen in urea (1452 cm^{-1}), creatinine (1490 cm^{-1}) and glucose (1074 cm^{-1}). For each set the amplitude of second derivative vibrational mode is plotted for 1452 cm^{-1} (A), 1490 cm^{-1} (B) and 1074 cm^{-1}(C), along with the ROC curve analysis to discriminate ND and D + I from D rats, and Pearson correlations between: urinary creatinine and amplitude of 1452 cm^{-1} (A); urinary creatinine and amplitude of 1490 cm^{-1} (B); and glycosuria and amplitude of 1490 cm^{-1}.

1200–900 cm^{-1} and the absorption bands for many of these compounds are C—H stretches and bonds, O—H bonds, and C—C stretches which can overlap [35,36]. Although the spectra of these monosaccharides are very similar with glucose, some differences in the absorption frequency occur between glucose and with fructose, galactose, mannose, as previously described [36]. Therefore, our data therefore suggest that the vibrational modes at 1074 cm^{-1} may correspond to the more specific absorption of glucose compared to some model compound spectra.

Although the present study identified novel urinary infrared spectral biomarkers for screening and monitoring metabolic control of diabetes, further studies are needed to confirm these potential urinary biomarkers in humans and to evaluate the suitableness of ATR-FTIR platforms for the screening and monitoring diabetes in human urine. Another potential limitation of the present study is the use of diabetic animals which display higher levels of blood glucose concentration, which is a typical outcome in streptozotocin-induced diabetic rats. Another limitation of urine samples are the changes in urinary components during the day due to changes in hydric behavior and glycemic variation, which can restrict the detection of acute metabolic modulation. We believe that these variations can be captured within the multivariate models and compensate the changes in urinary components.

The potential applications of ATR-FTIR using dried urine is necessary due to the strong absorption bands of water in infrared spectroscopy. Although the lyophilization of urine is not a fast procedure, it can be easily implemented in biomedical laboratories. Besides, the present analysis with dried biofluid samples can be brought into play in order to open up new perspectives to application in liquid samples directly dried in silicon internal reflection elements [9], low-cost aluminum foil substrates [37] or dried for 2 min directly onto the ATR crystal [7]. In this context, the present biophotonic approach coupled with unique univariate, multivariate, and learning machine analysis can indicate the presence of urinary glucose which can be determinant to perform a non-invasive screening method for diabetes.

4. Conclusion

In this study, ATR-FTIR spectroscopy was used to evaluate the urinary spectral differences between non-diabetics and insulin-treated diabetic than diabetic rats. The ATR-FTIR mean spectral analysis exhibited consistent changes related to urea, creatinine, and glucose from ND and D + I than D rats. PCA demonstrated discrimination between the ATR-FTIR spectra of urine with 99 % of the cumulative

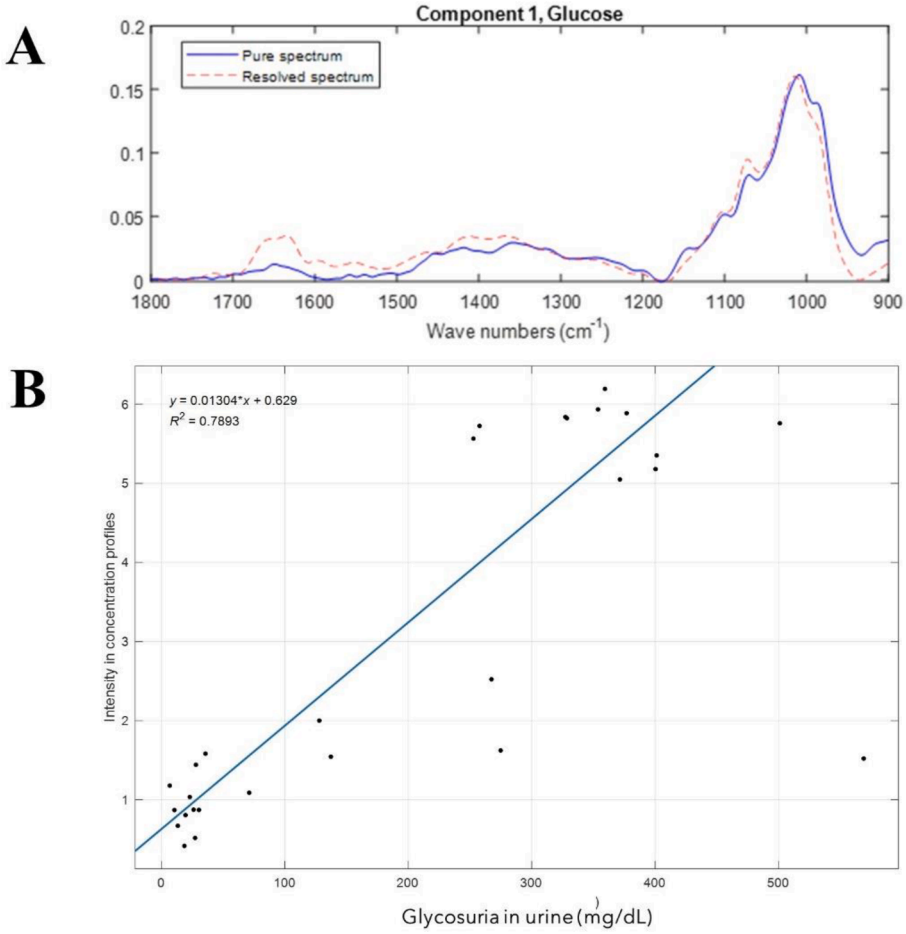

Fig. 6. FTIR spectra of laboratory-grade commercial glucose (blue line) and resolved spectrum obtained through MCR-ALS (dashed red line) (A). Scatter plot of glucose concentration estimated by MCR-ALS plotted against glycosuria obtained via enzymatic kits (B).

variance of ND compared to D, and 98.3 % comparing all groups, including D + I. PCA loadings associated to PC1 indicated urine glucose as one of the components for this discrimination between groups. It was reinforced by the 100 % of accuracy to discriminate ND and D + I than D rats using the amplitude of second derivatives of glucose at 1074 cm^{-1} as well as by the strong correlation ($r = 0.865$; $p < 0.0001$) between this vibrational mode with glycosuria. MCR-ALS analyses were also efficient in predicting glucose in the urine with a high relation between glucose in urine by enzymatic kit.

In summary, these results indicate that ATR-FTIR spectroscopy with univariate or multivariate analysis has the potential to provide information about the status of glucose in urine as a novel noninvasive approach to diabetes screening and monitoring.

CRediT authorship contribution statement

Douglas Carvalho Caixeta: Conceptualization, Methodology, Validation, Formal analysis, Investigation, Data curation, Writing – original draft, Writing – review & editing, Visualization. **Cassio Lima:** Methodology, Validation, Formal analysis, Investigation, Data curation, Writing – original draft, Writing – review & editing, Visualization. **Yun Xu:** Methodology, Validation, Formal analysis, Investigation, Data curation, Writing – review & editing. **Marco Guevara-Vega:** Methodology, Validation, Formal analysis, Investigation, Data curation, Writing – review & editing. **Foued Salmen Espindola:** Methodology, Validation, Formal analysis, Investigation, Resources, Data curation, Writing – review & editing, Supervision. **Royston Goodacre:** Methodology, Validation, Formal analysis, Investigation, Resources, Data curation, Writing – review & editing, Supervision, Funding acquisition. **Denise Maria Zezell:** Methodology, Validation, Formal analysis, Investigation, Resources, Data curation, Writing – review & editing, Supervision, Funding acquisition. **Robinson Sabino-Silva:** Conceptualization, Validation, Formal analysis, Investigation, Resources, Data curation, Writing – review & editing, Visualization, Supervision, Project administration, Funding acquisition.

Declaration of Competing Interest

The authors declare that they have no known competing financial interests or personal relationships that could have appeared to influence the work reported in this paper.

Data availability

Data will be made available on request.

Acknowledgement

We would like to thank our collaborators at the Rodent Vivarium Network (REBIR-UFU). The funders had no role in study design, data collection, and analysis, decision to publish, or preparation of the manuscript. This research was supported by a grant from CAPES/CNPq (#88887.506792/2020-00), CNPq INCT n° 465763/2014-6, FAPEMIG (#APQ-02872-16 and APQ-02148-21), Federal University of Uberlandia and National Institute of Science and Technology in Theranostics and Nanobiotechnology (CNPq Process N.: 465669/2014-0 and N.: 403193/

2022-2). Caixeta, D.C. received a fellowship from FAPEMIG, Sabino-Silva, R and Lima, C.A. received a fellowship from PrInt CAPES/UFU and CNPq 141629/2015-0, respectively. Zezell, D.M. and Sabino-Silva, R also received a productivity fellowship CNPq.

References

[1] ADA, Classification and Diagnosis of Diabetes: Standards of Medical Care in Diabetes—2020, Diabetes Care, 43 (2019) S14-S31.
[2] IDF, International Diabetes Federation - Diabetes Atlas, 10th edn, in: International Diabetes Federation, Brussels, Belgium, 2021.
[3] S. Copur, E.M. Onal, B. Afsar, A. Ortiz, D.H. van Raalte, D.Z. Cherney, P. Rossing, M. Kanbay, Diabetes mellitus in chronic kidney disease: Biomarkers beyond HbA1c to estimate glycemic control and diabetes-dependent morbidity and mortality, J. Diabetes Complications 34 (2020), 107707.
[4] J. Wysocki, A. Goodling, M. Burgaya, K. Whitlock, J. Ruzinski, D. Batlle, M. Afkarian, Urine RAS components in mice and people with type 1 diabetes and chronic kidney disease, 313 (2017) F487-F494.
[5] T.O. Ilori, M.A. Blount, C.F. Martin, J.M. Sands, J.D. Klein, Urine concentration in the diabetic mouse requires both urea and water transporters, 304 (2013) F103-F111.
[6] Y. Li, J. Xu, X. Su, Analysis of urine composition in type II diabetic mice after intervention therapy using holothurian polypeptides, Front. Chem. 5 (2017) 54.
[7] D.C. Caixeta, E.M.G. Aguiar, L. Cardoso-Sousa, L.M.D. Coelho, S.W. Oliveira, F. S. Espindola, L. Raniero, K.T.B. Crosara, M.J. Baker, W.L. Siqueira, R. Sabino-Silva, Salivary molecular spectroscopy: a sustainable, rapid and non-invasive monitoring tool for diabetes mellitus during insulin treatment, PLoS One 15 (2020) e0223461.
[8] G. Theophilou, K.M. Lima, P.L. Martin-Hirsch, H.F. Stringfellow, F.L. Martin, ATR-FTIR spectroscopy coupled with chemometric analysis discriminates normal, borderline and malignant ovarian tissue: classifying subtypes of human cancer, Analyst 141 (2016) 585–594.
[9] H.J. Butler, P.M. Brennan, J.M. Cameron, D. Finlayson, M.G. Hegarty, M. D. Jenkinson, D.S. Palmer, B.R. Smith, M.J. Baker, Development of high-throughput ATR-FTIR technology for rapid triage of brain cancer, Nat. Commun. 10 (2019) 4501.
[10] M. Paraskevaidi, C.L.M. Morais, K.M.G. Lima, J.S. Snowden, J.A. Saxon, A.M. T. Richardson, M. Jones, D.M.A. Mann, D. Allsop, P.L. Martin-Hirsch, F.L. Martin, Differential diagnosis of Alzheimer's disease using spectrochemical analysis of blood, Proc. Natl. Acad. Sci. U. S. A. 114 (2017) E7929–E7938.
[11] D. Perez-Guaita, Z. Richardson, P. Heraud, B. Wood, Quantification and identification of microproteinuria using ultrafiltration and ATR-FTIR spectroscopy, Anal. Chem. 92 (2020) 2409–2416.
[12] M. Steenbeke, S. De Bruyne, J. Boelens, M. Oyaert, G. Glorieux, W. Van Biesen, J. Linjala, J.R. Delanghe, M.M. Speeckaert, Exploring the possibilities of infrared spectroscopy for urine sediment examination and detection of pathogenic bacteria in urinary tract infections, Clin. Chem. Lab. Med. 58 (2020) 1759–1767.
[13] M. Paraskevaidi, C.L.M. Morais, K.M.G. Lima, K.M. Ashton, H.F. Stringfellow, P. L. Martin-Hirsch, F.L. Martin, Potential of mid-infrared spectroscopy as a non-invasive diagnostic test in urine for endometrial or ovarian cancer, Analyst 143 (2018) 3156–3163.
[14] Z. Guleken, H. Bulut, J. Depciuch, N. Tarhan, Diagnosis of endometriosis using endometrioma volume and vibrational spectroscopy with multivariate methods as a noninvasive method, Spectrochim. Acta A Mol. Biomol. Spectrosc. 264 (2022), 120246.
[15] D.K.R. Medipally, T.N.Q. Nguyen, J. Bryant, V. Untereiner, G.D. Sockalingum, D. Cullen, E. Noone, S. Bradshaw, M. Finn, M. Dunne, A.M. Shannon, J. Armstrong, F.M. Lyng, A.D. Meade, Monitoring radiotherapeutic response in prostate cancer patients using high throughput FTIR spectroscopy of liquid biopsies, Cancers (Basel) (2019) E925.
[16] H. Qian, X. Shao, H. Zhang, Y. Wang, S. Liu, J. Pan, W. Xue, Diagnosis of urogenital cancer combining deep learning algorithms and surface-enhanced Raman spectroscopy based on small extracellular vesicles, Spectrochim. Acta A Mol. Biomol. Spectrosc. 281 (2022), 121603.
[17] A. Fanelli, S. Rapi, S. Dugheri, A. Bonari, E. Milletti, G. Cappelli, N. Mucci, G. Arcangeli, Identification of amoxicillin crystals in urine: a case report, Clin. Lab. 66 (2020).
[18] Y. Du, V.B. Roger, J. Mena, M. Kang, M.L. Stoller, S.P. Ho, Structural and chemical heterogeneities of primary hyperoxaluria kidney stones from pediatric patients, J. Pediatr. Urol. 17 (214) (2021) 214.e211.
[19] V. Balan, C.T. Mihai, F.D. Cojocaru, C.M. Uritu, G. Dodi, D. Botezat, I. Gardikiotis, Vibrational spectroscopy fingerprinting in medicine: from molecular to clinical practice, Materials (Basel Switzerland) 12 (2019).
[20] R. Sabino-Silva, H.S. Freitas, M.L. Lamers, M.M. Okamoto, M.F. Santos, U. F. Machado, Na+-glucose cotransporter SGLT1 protein in salivary glands: potential involvement in the diabetes-induced decrease in salivary flow, J. Membr. Biol. 228 (2009) 63–69.
[21] D. Diniz Vilela, L. Gomes Peixoto, R.R. Teixeira, N. Belele Baptista, D. Carvalho Caixeta, A. Vieira de Souza, H.L. Machado, M.N. Pereira, R. Sabino-Silva, F.S. Espindola, The Role of Metformin in Controlling Oxidative Stress in Muscle of Diabetic Rats, Oxidative medicine and cellular longevity, 2016 (2016) 6978625.
[22] L.G. Peixoto, R.R. Teixeira, D.D. Vilela, L.N. Barbosa, D.C. Caixeta, S.R. Deconte, F. de Assis, R. de Araújo, F.S.E. Sabino-Silva, Metformin attenuates the TLR4 inflammatory pathway in skeletal muscle of diabetic rats, Acta Diabetol. 54 (2017) 943–951.
[23] A. Subaihi, L. Almanqur, H. Muhamadali, N. AlMasoud, D.I. Ellis, D.K. Trivedi, K. A. Hollywood, Y. Xu, R. Goodacre, Rapid, accurate, and quantitative detection of propranolol in multiple human biofluids via surface-enhanced raman scattering, Anal. Chem. 88 (2016) 10884–10892.
[24] R. Sabino-Silva, A.B. Alves-Wagner, K. Burgi, M.M. Okamoto, A.S. Alves, G. A. Lima, H.S. Freitas, V.R. Antunes, U.F. Machado, SGLT1 protein expression in plasma membrane of acinar cells correlates with the sympathetic outflow to salivary glands in diabetic and hypertensive rats, American journal of physiology, Endocrinol. Metab. 299 (2010) E1028–E1037.
[25] H.S. Freitas, B.D. Schaan, A. David-Silva, R. Sabino-Silva, M.M. Okamoto, A. B. Alves-Wagner, R.C. Mori, U.F. Machado, SLC2A2 gene expression in kidney of diabetic rats is regulated by HNF-1α and HNF-3β, Mol. Cell. Endocrinol. 305 (2009) 63–70.
[26] H.S. Freitas, B. D'Agord Schaan, R.S. da Silva, M.M. Okamoto, M. Oliveira-Souza, U.F. Machado, Insulin but not phlorizin treatment induces a transient increase in GLUT2 gene expression in the kidney of diabetic rats, Nephron Physiol. 105 (2007) p42–p51.
[27] R. Keuleers, H.O. Desseyn, B. Rousseau, C. Van Alsenoy, Vibrational analysis of urea, Chem. A Eur. J. 103 (1999) 4621–4630.
[28] R.A. Shaw, S. Low-Ying, M. Leroux, H.H. Mantsch, Toward reagent-free clinical analysis: quantitation of urine urea, creatinine, and total protein from the mid-infrared spectra of dried urine films, Clin. Chem. 46 (2000) 1493–1495.
[29] K.V. Oliver, A. Maréchal, P.R. Rich, Effects of the hydration state on the mid-infrared spectra of urea and creatinine in relation to urine analyses, Appl. Spectrosc. 70 (2016) 983–994.
[30] M. Khajehpour, J.L. Dashnau, J.M. Vanderkooi, Infrared spectroscopy used to evaluate glycosylation of proteins, Anal. Biochem. 348 (2006) 40–48.
[31] D. Simonova, I. Karamancheva, Application of fourier transform infrared spectroscopy for tumor diagnosis, Biotechnol. Biotechnol. Equip. 27 (2013) 4200–4207.
[32] C.B. Parker, E.R. DeLong, ROC methodology within a monitoring framework, Stat. Med. 22 (2003) 3473–3488.
[33] H.Y. Dong, J. Xie, L.H. Chen, T.T. Wang, Y.R. Zhao, Y.L. Dong, Therapeutic drug monitoring and receiver operating characteristic curve prediction may reduce the development of linezolid-associated thrombocytopenia in critically ill patients, Eur. J. Clin. Microbiol. Infect. Dis. 33 (2014) 1029–1035.
[34] M.J. Müller, B. Regenbogen, S. Härtter, F.X. Eich, C. Hiemke, Therapeutic drug monitoring for optimizing amisulpride therapy in patients with schizophrenia, J. Psychiatr. Res. 41 (2007) 673–679.
[35] Z. Movasaghi, S. Rehman, D.I. ur Rehman, Fourier Transform Infrared (FTIR) Spectroscopy of Biological Tissues, Applied Spectroscopy Reviews, 43 (2008) 134-179.
[36] C. Petibois, V. Rigalleau, A.-M. Melin, A. Perromat, G. Cazorla, H. Gin, G.r. Déléris, Determination of Glucose in Dried Serum Samples by Fourier-Transform Infrared Spectroscopy, Clinical chemistry, 45 (1999) 1530-1535.
[37] M. Paraskevaidi, C.L.M. Morais, O. Raglan, K.M.G. Lima, E. Paraskevaidis, P. L. Martin-Hirsch, M. Kyrgiou, F.L. Martin, Aluminium foil as an alternative substrate for the spectroscopic interrogation of endometrial cancer, J. Biophotonics 11 (2018) e201700372.